The role of diffusion on the products of cool laminar n-heptane/air premixed flames

K. Lam[1], A. Wehrfritz[1], E. R. Hawkes[1,2] and B. Savard[1]

[1]School of Mechanical and Manufacturing Engineering
University of New South Wales, Sydney, NSW 2052, Australia

[2]School of Photovoltaic and Renewable Energy Engineering
University of New South Wales, Sydney, NSW 2052, Australia

Abstract

Many practical engines feature regimes in which a two-stage ignition behavior is observed, wherein a first low-temperature chemistry ignition (a cool flame) is followed by a second high-temperature chemistry ignition. The present numerical study explores the role of diffusion on cool flame propagation and second-stage ignition by analysing n-heptane premixed laminar flames within the two-stage ignition regime. The selected conditions consist of an n-heptane/air mixture at a temperature of 650 K, pressure of 1 atmosphere and equivalence ratio of 0.7. These conditions were selected to produce a significant delay between first- and second-stage ignitions for easy isolation of the cool flame used in the present analysis. Steady-state, laminar freely propagating cool flames were simulated over a specified domain with varying inflow velocities. Comparison of the cool flame structure response to varying inflow velocity showed that: 1) the temperature, heat release rate and mass fraction profiles approach the zero-dimensional solution with increasing inflow velocity, i.e. as the relative importance of diffusion decreases, and 2) at lower inlet velocities the cool flame products become highly sensitive to inflow velocity. It is found that the latter result has an important consequence: the remaining time to second-stage ignition in these products is significantly affected, such that it is an order of magnitude larger than in pure zero-dimensional ignition for velocities near the cool flame deflagration speed. This result has important consequences for homogeneous charge compression-ignition and diesel spray flame modeling, as the ignition delay time in the products of cool flames can strongly affect the occurrence of knock in the former and hot flame stabilisation in the latter. Finally, it is shown that diffusion, as opposed to differential diffusion, is responsible for the effects observed as results obtained with two transport models (neglecting and accounting for differential diffusion effects, respectively) show similar trends.

Introduction

An intrinsic feature of many large hydrocarbons present in high concentration in transportation fuels (e.g. long chained alkanes in diesel, kerosene, gasoline, etc.) is their two-stage ignition behavior over a wide range of operating conditions [1]. This is characterised by low-temperature chemistry (LTC) reactions inducing the first-stage ignition (a cool flame) with low heat release rates and minimal CO_2 production [1, 2, 3, 4]. The cool flame contains highly reactive radicals and intermediate species like formaldehyde (CH_2O) [5], which promote the onset of high-temperature chemistry (HTC) reactions leading to the final, second-stage ignition with large heat release [1, 2, 3]. Improved control over the in-cylinder combustion processes of internal combustion engines to reduce pollutant emissions and improve fuel efficiency has necessitated the renewed interest in cool flames in recent years [6, 7]. For example, cool flames are known to be a cause for knock in spark ignition engines, thus preventing the use of high compression ratios for improved engine efficiency [7]. In compression ignition engines, cool flames initiate the ignition sequence [6] and play a significant role in the stabilisation of diesel flames [8]. Controlling the timing of ignition and flame stabilisation has determining impact on the engine performance in terms of power, efficiency, and pollutant emissions. This can be achieved in part through an improved understanding of cool flames.

Studies of cool flames have been performed on non-premixed [9, 5] and premixed [2] flames in counter flow configurations and freely propagating premixed flames [3, 10, 11, 2, 12, 4]. A recent numerical study by Zhang et al. [3] demonstrated that cool flames have a significant effect on hot flame propagation. The study was on the transient evolution of premixed dimethyl ether (DME)/air cool flames and found that within a certain temperature range cool flames could be initiated from a hotspot. HTC autoignition from the centre of the hotspot resulted in double flame structures consisting of leading cool flames and trailing hot flames. Eventually the hot flames joined with the cool flames due to their faster front speed producing flames with greater propagating speeds than their single hot flame counterparts. It was found that equivalence ratio, initial temperature and oxygen concentration were controlling factors in cool flame speed and duration. Ju et al. [10] also observed double flame structures when investigating freely propagating flames of DME/oxygen mixtures within the negative temperature coefficient (NTC) region. It was concluded that the presence of cool flames significantly extend the flammability limit. Liang and Law [11] found similar agreement in their numerical study on flammability limits of n-heptane/air mixtures. In another study, Zhao et al. [2] demonstrated numerically the significance of LTC by observing the temperature and heat release rate profiles of laminar premixed flames at temperatures within and above the NTC regime.

An aspect that has received limited attention is the role of diffusion on premixed cool flames. In the limit of pure autoignition waves, diffusion plays a negligible role and convection balances LTC reactions, with propagation controlled by the residence time of the incoming reactants. In contrast, in the deflagration limit, diffusion of heat and radicals from the products/reaction zone to the reactants sustains the cool flame propagation. Both types of flames have been identified numerically [10, 4, 2, 3] and experimentally [12, 2]. While the role of diffusion on cool flame propagation speeds has been studied [12, 2, 3], its effect on the flame structure remains poorly understood. In a recent numerical study, Savard et al. [13] observed that the products of a lean n-heptane/air cool flame at atmospheric pressure are significantly affected by the transition from one propagation limit to the other. However, it is unclear if this effect is 1) specific to the chemical mechanism used in that study, 2) attributable to differential diffusion (as opposed to diffusion in general), and 3) important with respect to the remaining time to second-stage ignition. The present paper addresses each of these points.

Specifically, the objective of the current study is to investigate numerically the role of diffusion on cool flame propagation and

its subsequent effect on second-stage ignition. The focus is on a premixed *n*-heptane/air mixture within the NTC regime. The paper is organised as follow. First, the methodology is presented. Then, the results of the cool flame structure are presented and the implications of those results on the time to second-stage ignition are discussed.

Methodology

The approach taken in the current study is to simulate steady state, laminar freely propagating *n*-heptane/air premixed flames using two different molecular transport models. The domain is selected to isolate the cool flame for analysis. Three chemical kinetic mechanisms are considered to verify the consistency of the results obtained. Details of the transport models, chemical mechanisms, and the simulation set-up are presented next.

Transport models

The mixture-averaged and unity Lewis number transport models are considered to assess the role of differential diffusion on cool flame products. Within the mixture-averaged model the diffusive mass flux of a species k is expressed by

$$J_k = \rho \left[-\frac{W_k}{W} D_{k,m} \nabla X_k + Y_k \left(\sum \frac{W_k}{W} D_{k,m} \nabla X_k \right) \right] \quad (1)$$

$$D_{k,m} = \frac{1 - Y_k}{\sum_{j \neq k} \frac{X_j}{\mathcal{D}_{k,j}}} \quad (2)$$

where X_k, Y_k, W_k, and $D_{k,m}$ are the molar fraction, mass fraction, molecular weight and mixture-averaged binary diffusion coefficient for species k, respectively, ρ is the density, and W is the mixture molecular weight. $\mathcal{D}_{k,i}$ is the binary diffusion coefficient of species k into species j.

With the unity Lewis number model the mass diffusion coefficients are set equal to the thermal diffusion coefficient, i.e. $Le_k = \alpha / D_{k,m} = 1$. The diffusive mass flux thus simplifies to $J_k = -\rho \alpha \nabla Y_k$.

Chemical kinetic mechanisms

Three reduced mechanisms that included both LTC and HTC *n*-heptane/air chemistry are considered: the mechanism by Yoo et al. [14], containing 88 species and 387 reactions, Caltech-Mech [15], containing 129 species (aromatic species removed from the full mechanism due to the lean conditions considered here) and 1234 reactions, and the Polimi mechanism [16], containing 100 species and 1738 reactions. Figure 1 presents the 0D ignition delay as a function of inverse of temperature obtained at constant pressure of 1 atm and equivalence ratio of 0.7. LTC (first-stage) and HTC (second-stage) ignition are identified by the peak in $C_7H_{15}O_2$ (RO_2) and OH mass fractions, respectively [17, 18]. The NTC region is clearly reproduced by all three mechanisms.

Simulation set-up

The present study considers an *n*-heptane/air mixture with equivalence ratio of 0.7 at constant pressure of 1 atmosphere and initial temperature of 650 K. These initial conditions are selected to observe the effect of two-stage ignition within the NTC region. Further the conditions are selected such that there is a significant delay between first-stage and second-stage ignition to enable effective isolation of the cool flame, as demonstrated in Fig. 1 where the time to second-stage ignition is significantly larger than the first-stage ignition delay. The conditions also coincide with those used in [13].

One-dimensional inflow/outflow domains are considered to simulate the cool flames. A specified domain size is required
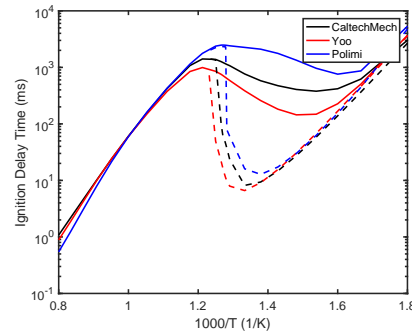

Figure 1: 0D ignition delay time for *n*-heptane/air at constant pressure (1 atm) and equivalence ratio of 0.7. Solid lines: ignition delay time. Dotted lines: first-stage ignition times

to isolate the cool flames in the absence of HTC. The domain length is set so that the total flow residence time is approximately 80 ms, which is within the bounds of first- and second-stage ignitions obtained from the 0D calculations. The residence time is defined as $t_{res}(x) = \int_0^x dx/u(x)$, where u is the local velocity. This ensures enough time for LTC reactions to take place before HTC reactions dominate. To accurately resolve the cool flame, a grid spacing of 10–50 μm is used (more than 20 grid points per reactive species layers).

For each transport model/chemical mechanism pair, the inflow velocity is varied (effectively varying the contribution from diffusion) to cover the transition from autoignition waves to attached flames, including the deflagration regime. For each inflow velocity, the simulation is run until a steady state is reached. The simulations are performed with Cantera, using the burner-stabilised flame configuration [19]. The cool flames are initialised with the 0D solution assuming constant mass flow rate, advanced in time until a steady state is reached (in-house modification of the Cantera solver), before being fed to the steady state solver to ensure correct convergence to the steady cool flame solution.

Results and Discussion

The results for the cool flame structure obtained with the mixture-averaged transport model are presented first followed by results obtained with the unity Lewis number model. Only the the results obtained with the Yoo mechanism are included for brevity (similar structure obtained with other mechanisms). The effect of varying inflow velocity on the remaining time to second-stage ignition in the cool flame products is then presented for all three mechanisms.

Cool flame structure

The change in the structure of the laminar cool flames obtained using the mixture-averaged transport model is shown in Fig. 2, together with the 0D homogenous solution. Looking first at the 0D solution, an exponential increase in heat release rate and mass fraction of the $C_7H_{15}O_2$ radical is observed until most of the fuel is rapidly consumed and formaldehyde is produced just before 70 ms, completing first-stage ignition.

The profiles of the 1D laminar flames correspond to inlet velocities less than, at and above the reference laminar cool flame speed $S_R = 0.26 m/s$. This reference deflagration speed was obtained as in [13] using the method proposed by Krisman et al. [20]. The flame position moves downstream with increasing inflow velocity (both in residence time and physical space) and the profiles approach the 0D solution. This is attributable
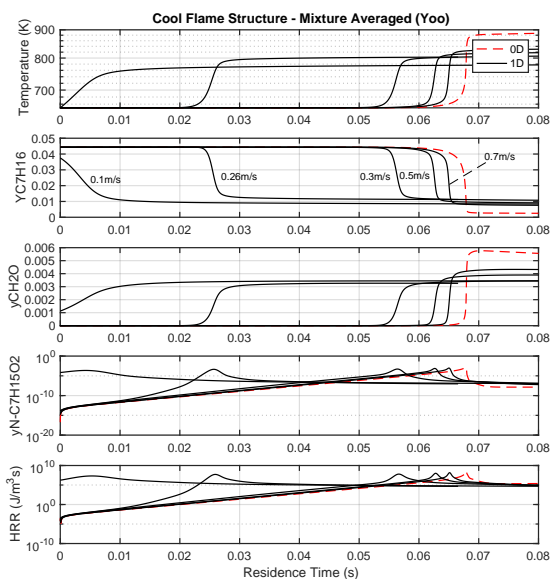
Figure 2: Cool flame structure at varying inflow velocities using mixture-averaged transport. $S_R = 0.26$ m/s.

Figure 3: Cool flame structure at varying inflow velocity using unity Lewis number transport. $S_R = 0.33$ m/s.

to the decreased contribution of diffusion with high inflow velocity, as was shown in [13] for the present flames (but with CaltechMech). Another important effect of varying inflow velocity (or the contribution from diffusion) is observed in the cool flame products: temperature and species concentrations are strongly sensitive to inflow velocity. Figure 3 presents the results for laminar flames with unity Lewis number (where differential diffusion is absent). As in the mixture-averaged case the cool flame products are highly sensitive to inflow velocity (for inflow velocities of the order of S_R). The similarity of trends observed with both transport models suggests that the observed phenomena cannot be solely attributed to differential diffusion, but rather diffusion in general.

In this section, a strong effect of the propagation regime (ignition front vs. deflagration) on the cool flame products has been observed independently of the transport model. The observed variations in these products may have important effects on the reactivity of the subsequent HTC reactions, which, in an engine, would follow the cool flame. This potential importance is assessed next.

Remaining time to second-stage ignition

The effect of inflow velocity on the remaining time to ignition was examined by extracting the species mass fractions and temperature from the laminar flame solutions at a residence time of 80 ms. These were applied as initial conditions to calculate the remaining time to second-stage ignition (t_{12}) using an ideal gas constant pressure homogeneous reactor (0D).

The remaining time to second-stage ignition for the unity and non-unity Lewis number cool flames are depicted in Fig. 4(a) and compared to the complete 0D solution (red dashed lines in Fig. 2 and 3). The graph shows an asymptotic decline of the remaining time to second-stage ignition with increasing inflow velocity. Also, the sensitivity of the cool flame to low velocities is demonstrated here where it is shown to retard the remaining ignition delay time by an order of magnitude larger than the homogenous solution. There is only a minor disparity between times obtained for unity Lewis number and mixture-averaged transport.
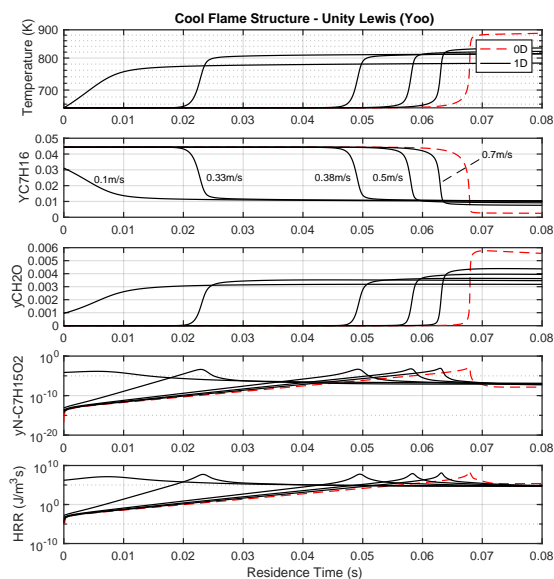
Finally, Fig. 4(b) presents similar results for all three chemical mechanisms, considering only the unity Lewis number cases. Here, the inflow velocity is normalized by the respective reference laminar flame speed. The y-axis corresponds to the increase in t_{12} with respect to the complete 0D solution, $t_{12,0D}$, normalized by the 0D first-stage ignition delay ($t_{1,0D}$). Similar qualitative results are obtained independently of the mechanisms. Figure 4(b) indicates that for the conditions tested, a cool flame deflagration, as opposed to 0D ignition or a fast ignition wave, will increase the remaining time to HTC ignition in its products by 5–10 times the LTC ignition delay.

Conclusions

In this study, we investigated the role of diffusion on cool flame propagation through the consideration of laminar premixed cool n-heptane/air flames using mixture-averaged and unity Lewis number transport models and three chemical mechanisms. First, freely propagating cool flames were simulated in isolation of the hot flame at varying inflow velocities corresponding to values above, at and below the laminar reference flame speed. The thermochemical conditions at a fixed residence time in the cool flame products were taken to calculate the remaining time to second-stage ignition. The major findings of the study are:

- As the relative importance of diffusion decreases with increasing inflow velocity, it was found that the temperature, heat release rate and mass fraction profiles approached the zero-dimensional solution with increasing inflow velocity, consistent with previous hot flame studies.

- Cool flame products are highly sensitive to inflow velocities (at values of the order of the reference flame speed).

- This result was found to significantly impact the remaining time to second-stage ignition.

- Similar trends were observed across both transport models, disproving differential diffusion to be the sole cause of the observed behaviour.

- Similar results were consistently obtained with three different chemical mechanisms.

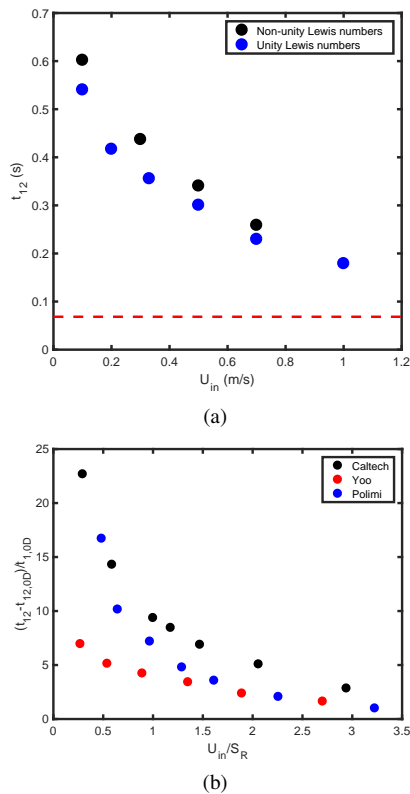The observed phenomenon may have important implications in

(a)

(b)

Figure 4: Delay time to second-stage ignition computed using temperature and species mass fraction conditions at 80 ms residence time with the Yoo mechanism (a) and all mechanisms (normalisation described in the main text) (b). Red dashed line: 0D homogenous solution.

spark ignition and compression ignition engines, in which cool flames are know to occur and where a precise control of the ignition timing is desired.

Acknowledgements

References

[1] F. L. Dryer. Chemical kinetic and combustion characteristics of transportation fuels. *Proc. Comb. Inst.*, 35:117–144, 2015.

[2] P. Zhao, W. Liang, S. Deng, and C. K. Law. Initiation and propagation of laminar premixed cool flames. *Fuel*, 166:477–487, 2016.

[3] W. Zhang, M. Faqih, X. Gou, and Z. Chen. Numerical study on the transient evolution of a premixed cool flame. *Combust. Flame*, 187:129–136, 2018.

[4] J. Pan, H. Wei, G. Shu, Z. Chen, and P. Zhao. The role of low temperature chemistry in combustion mode development under elevated pressures. *Combust. Flame*, 174:179–193, 2016.

[5] C. B. Reuter, S. H. Won, and Y. Ju. Flame structure and ignition limit of partially premixed cool flames in a counterflow burner. *Proc. Comb. Inst.*, 36(1):1513–1522, 2017.

[6] M. P. B. Musculus, P. C. Miles, and L. M. Pickett. Conceptual models for partially premixed low-temperature diesel combustion. *Prog. Energy Combust. Sci.*, 39:246–283, 2013.

[7] J. M. Bergthorson and M. J. Thomson. A review of the combustion and emissions properties of advanced transportation biofuels and their impact on existing and future engines. *Renew. Sust. Energ. Rev.*, 42:1393–1417, 2015.

[8] L. M. Pickett, D. L. Siebers, and C. A. Idicheria. Relationship between ignition processes and the lift-off length of diesel fuel jets. In *Powertrain and Fluid Systems Conference and Exhibition*. SAE International, oct 2005.

[9] A. Stagni, D. Brignoli, M. Cinquanta, A. Cuoci, A. Frassoldati, E. Ranzi, and T. Faravelli. The influence of low-temperature chemistry on partially-premixed counterflow n-heptane/air flames. *Combust. Flame*, 188:440–452, 2018.

[10] Y. Ju, C. B. Reuter, and S. H. Won. Numerical simulations of premixed cool flames of dimethyl ether/oxygen mixtures. *Combust. Flame*, 162(10):3580–3588, 2015.

[11] W. Liang and C. K. Law. Extended flammability limits of n-heptane/air mixtures with cool flames. *Combust. Flame*, 185:75–81, 2017.

[12] M. Hajilou, T. Ombrello, S.H. Won, and E. Belmont. Experimental and numerical characterization of freely propagating ozone-activated dimethyl ether cool flame. *Combust. Flame*, 176:326–333, 2017.

[13] B. Savard, H. Wang, A. Teodorczyk, and E. R. Hawkes. Low-temperature chemistry in n-heptane/air premixed turbulent flames. *Combust. Flame*, 196:71–84, 2018.

[14] C. S. Yoo, T. Lu, J. H. Chen, and Chung K. Law. Direct numerical simulations of ignition of a lean n-heptane/air mixture with temperature inhomogeneities at constant volume: Parametric study. *Combust. Flame*, 158(9):1727–1741, 2011.

[15] G. Blanquart. CaltechMech v2.3. Available at http://theforce.caltech.edu/resources/.

[16] A. Stagni, A. Cuoci, A. Frassoldati, T. Faravelli, and E. Ranzi. Lumping and reduction of detailed kinetic schemes: An effective coupling. *Ind. Eng. Chem. Res.*, 53(22):9004–9016, 2014.

[17] A. Krisman, E. R. Hawkes, M. Talei, A. Bhagatwala, and J. H. Chen. Characterisation of two-stage ignition in diesel engine-relevant thermochemical conditions using direct numerical simulation. *Combust. Flame*, 172:326–341, 2016.

[18] S. S. Vasu, D. F. Davidson, Z. Hong, V. Vasudevan, and R. K. Hanson. n-Dodecane oxidation at high-pressures: Measurements of ignition delay times and OH concentration time-histories. *Proc. Comb. Inst.*, 1(32):173–180, 2009.

[19] D. G. Goodwin, H. K. Moffat, and R. L. Speth. Cantera: An object-oriented software toolkit for chemical kinetics, thermodynamics, and transport processes. http://www.cantera.org, 2017. Version 2.3.0.

[20] A. Krisman, E. R. Hawkes, and J. H. Chen. The structure and propagation of laminar flames under autoignitive conditions. *Combust. Flame*, 188:399–411, 2018.